Supporting Information for

Multi-Responsive Shape Memory and Self- Healing Hydrogels with Gold and Silver Nanoparticles

Hüsna Kılıç[a], Deniz Ceylan[b*]

[a]Bezmialem Vakıf University Health Sciences Institute, Department of Biotechnology, 34093 Istanbul, Turkey
[b]Bezmialem Vakif University, Faculty of Pharmacy, 34093 Istanbul, Turkey

[*]deniz.ceylan@bezmialem.edu.tr

Table of Contents

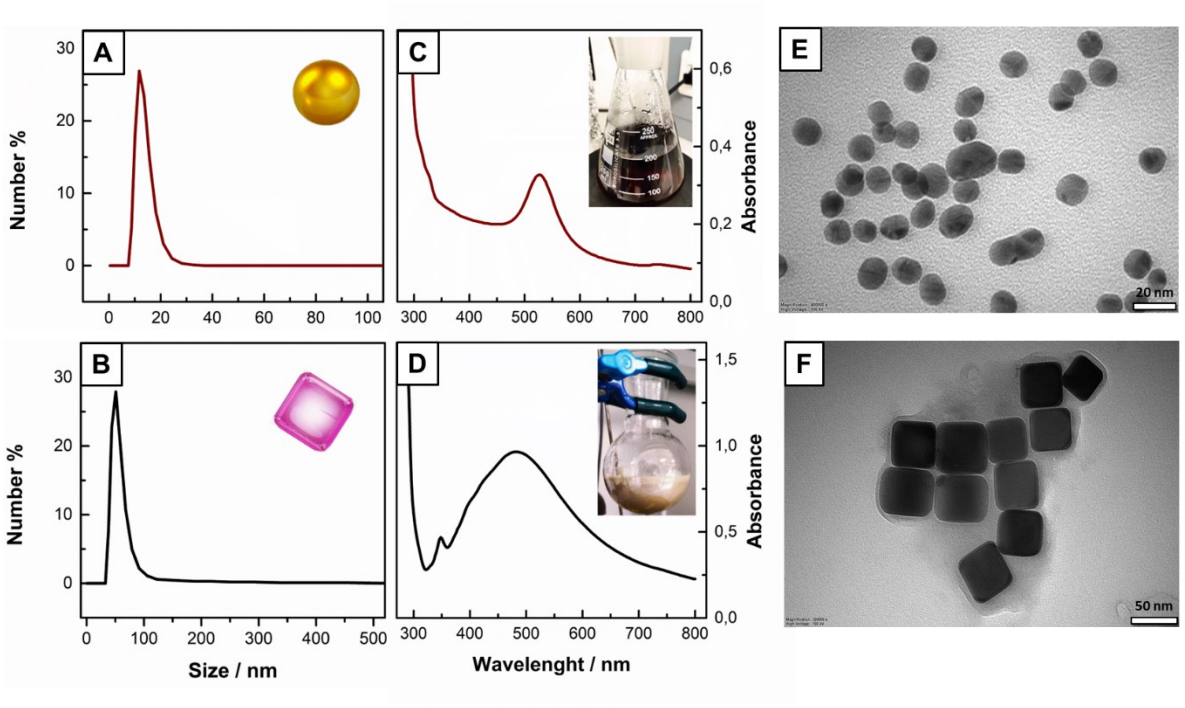

Figure S1. Characterization of PVP-coated gold nanosphere (AuNS@PVP) and silver nanocube (AgNC) particles in water **(A-B).** DLS measurement graph, **(C-D).** UV-Vis spectrum and **(E-F)**. TEM images obtained at 20x and 50x magnifications, respectively.

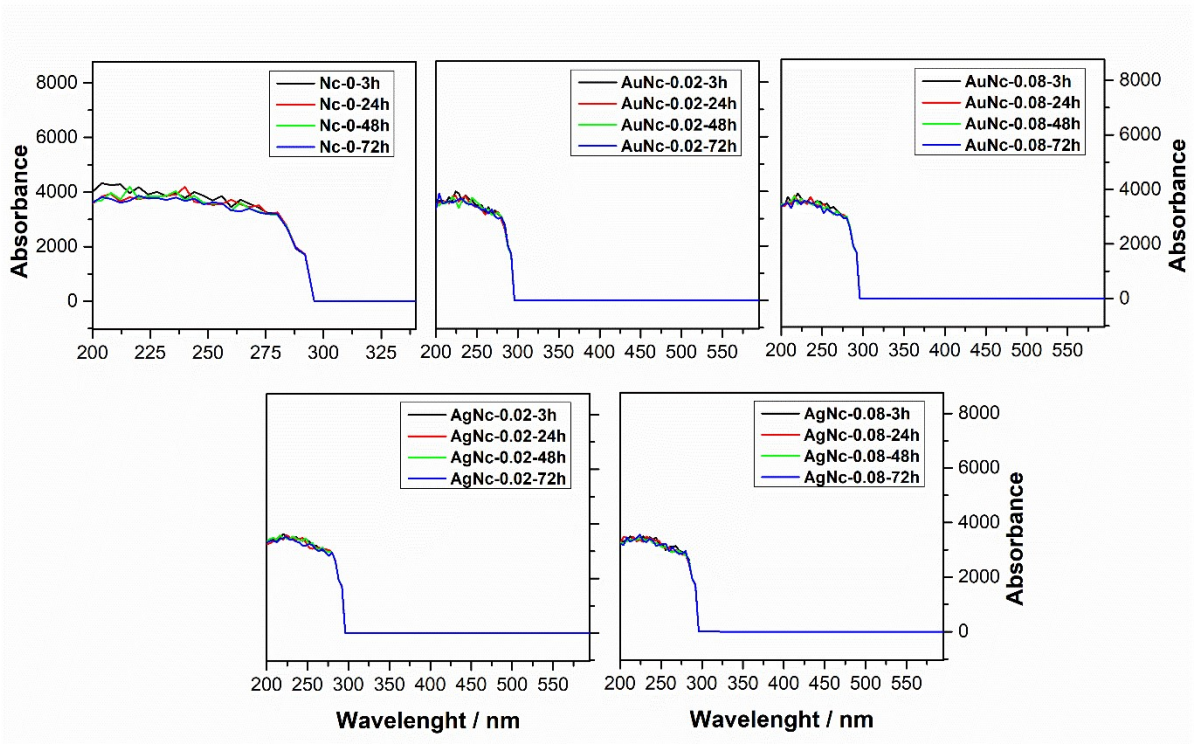

Figure S2. UV-Vis spectra of supernatants collected after immersion of Nc-0, Au/AgNc-x nanoparticle-loaded swollen hydrogels in water at different time intervals (3, 24, 48, and 72 hours).

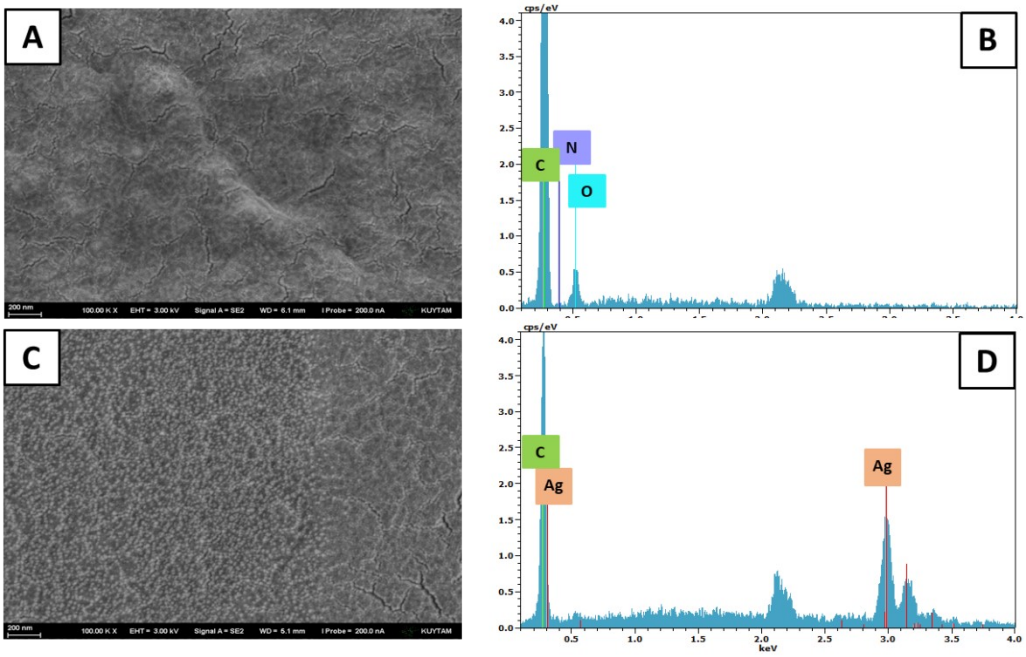

Figure S3. SEM images and EDX analysis results of Nc-0 (A and B) and AgNc-0.08 gels (C and D) after synthesis. The scale bars represent 200 nm.

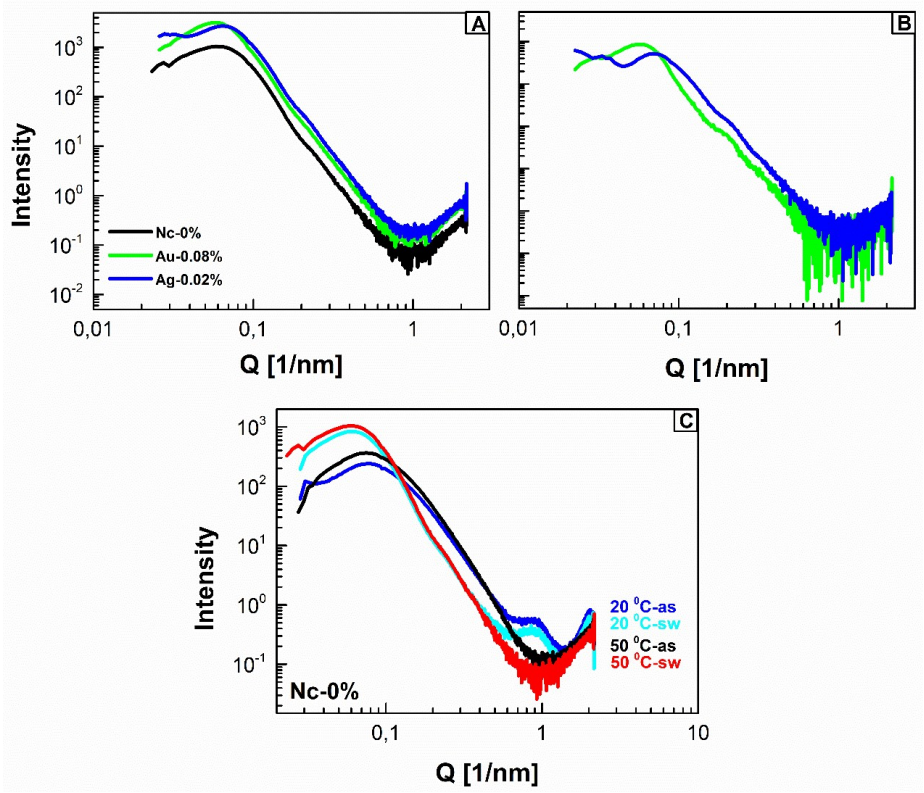

Figure S4. SAXS patterns at 50 ℃ of swollen **(A)** Nc-0, AuNc-0.08 and AgNc-0.02 gels **(B)** Nc-0 subtracted patterns of Au-0.08 and Ag-0.02 gels and **(C)** Nc-0 SAXS patterns of the gel obtained at 20 ℃ and 50 ℃ after synthesis and in the swollen state.

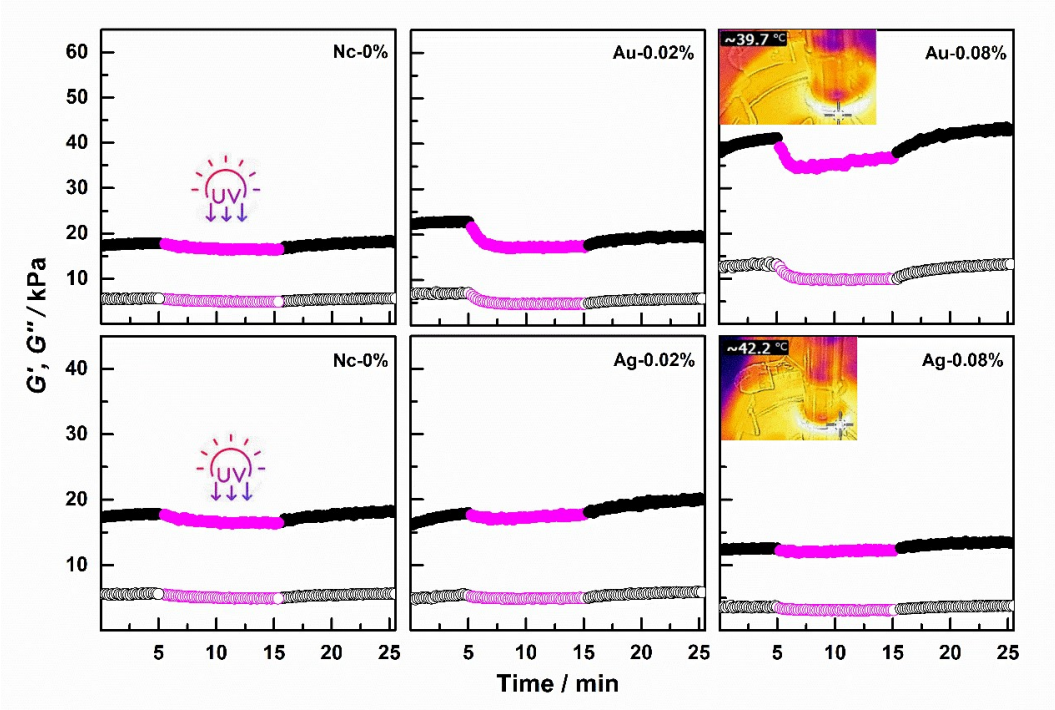

Figure S5. Time dependent variation of storage modulus (*G′*, filled symbols) and loss module (G″, open symbols) in swollen state Nc-0, AuNc-x and AgNC-x gels at 37 ℃ with and without UV using a UV light source of 365 nm, 200-700 nm and 400-500 nm, respectively.

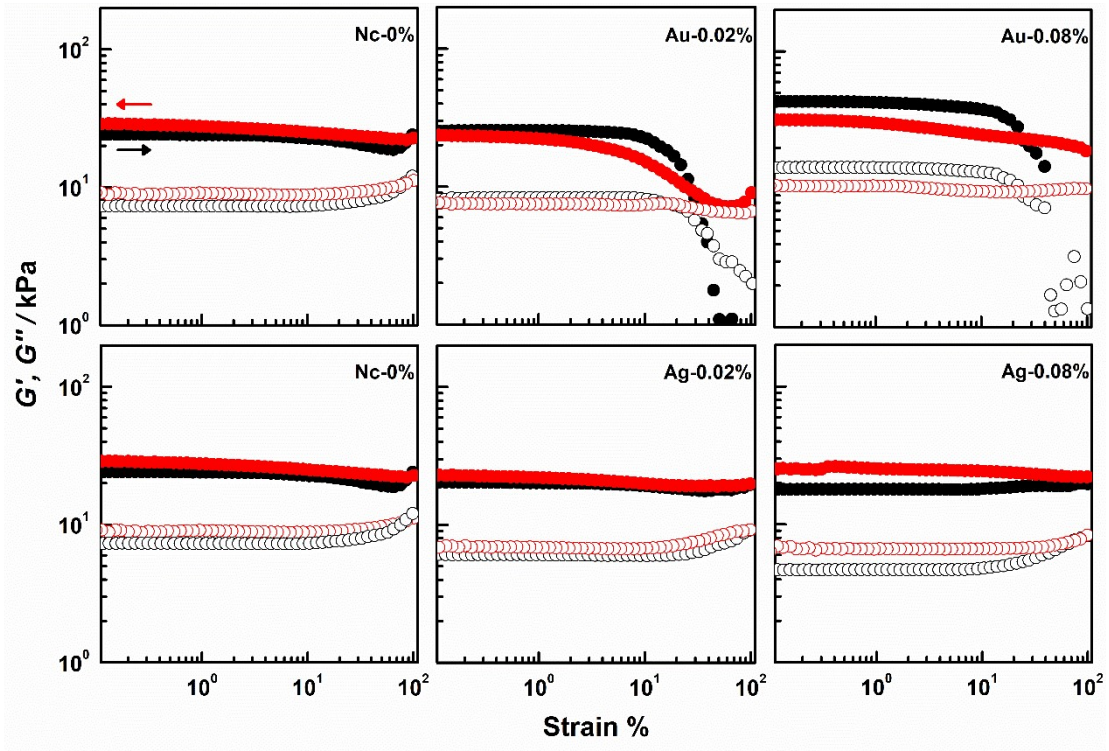

Figure S6. Deformation sweeps analysis of swollen state Nc-0, AuNc-x and AgNC-x networks. The deformation varied from 0.1% to 100% (black symbols) and 100% to 0.1% (red symbols) at a fixed frequency of 1 Hz at 37 ℃. The x values are indicated in the graphs, with storage module (G') filled symbols and loss module (G'') with open symbols.

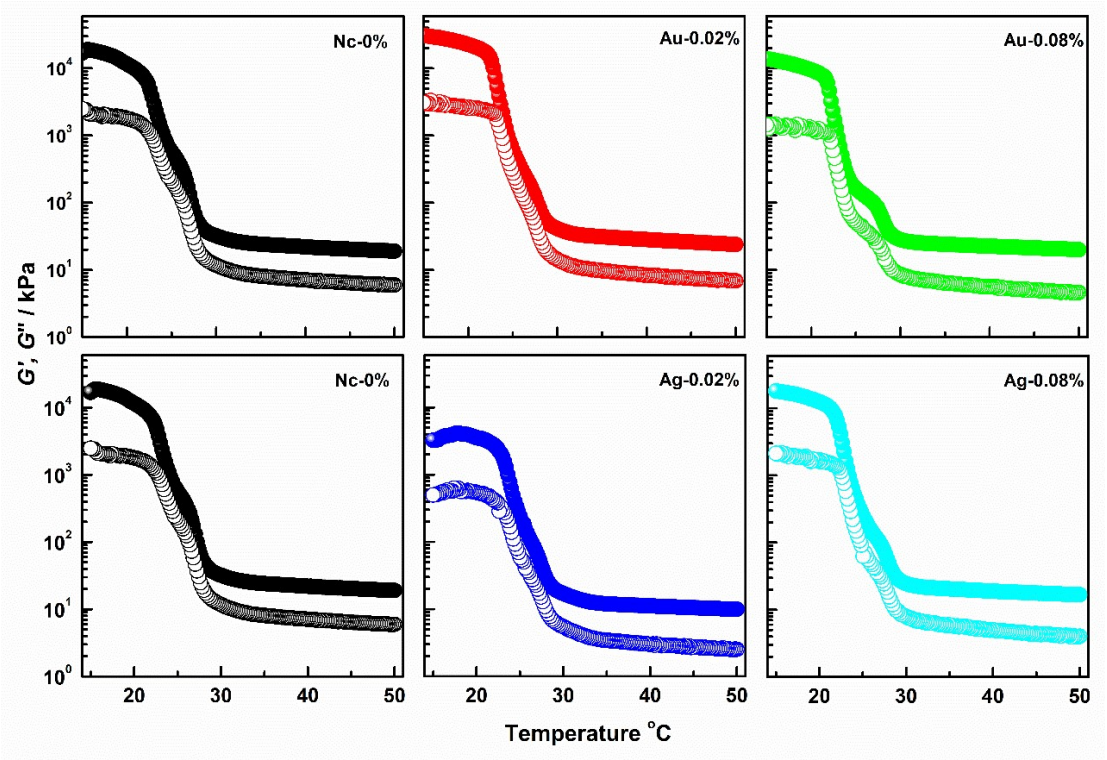

Figure S7. Temperature dependency of G' (filled symbols) and G'' (open symbols) for the swollen-sw state Nc-0, AuNc-x ve AgNC-x network.

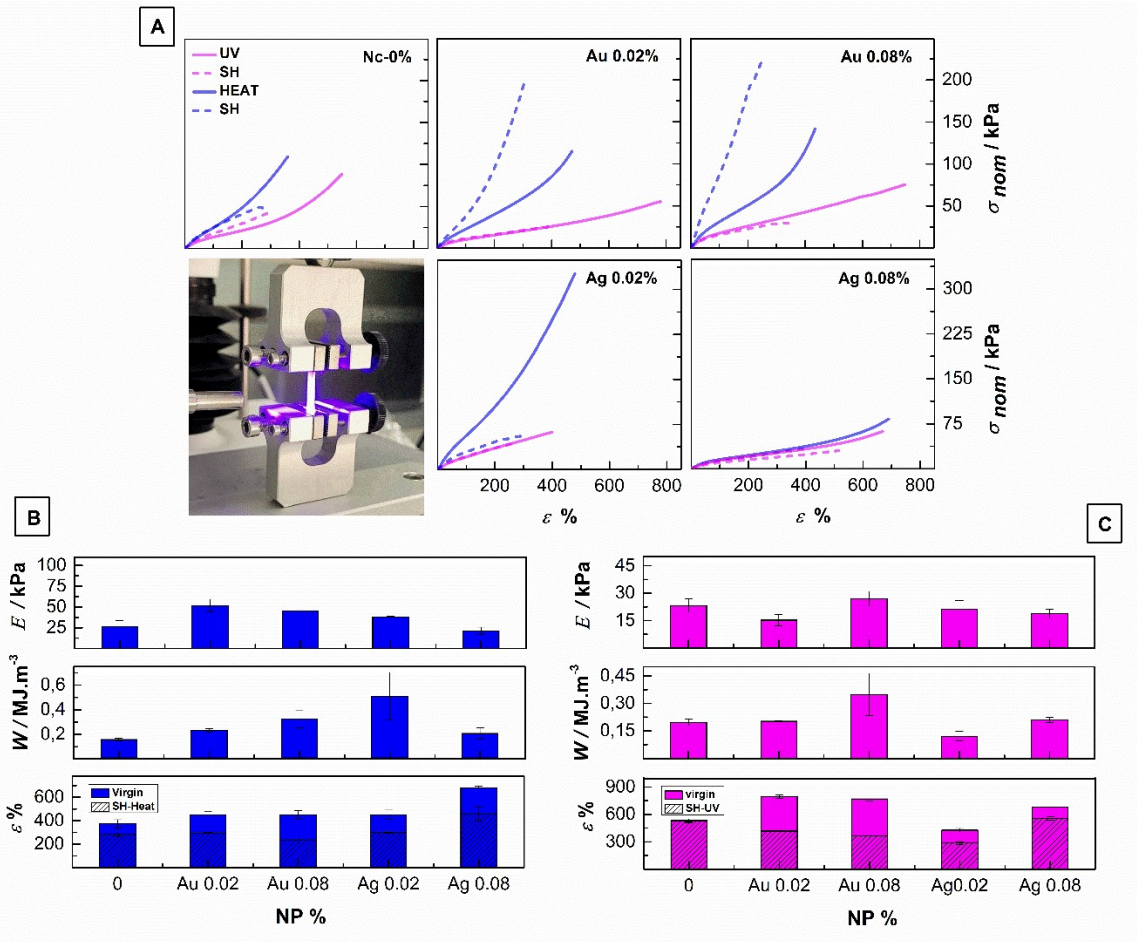

Figure S8. (A) Tensile stress-strain plots of virgin (blue and pink lines) and self-healed (SH-blue and pink dashed lines), Nc-0, AuNc-x and AgNc-x networks under temperature (blue) and appropriate UV light source (pink). **(B)** Young's modulus E, toughness W, fracture stress $\sigma_f$and elongation at break $\varepsilon\%$ as a function of temperature (blue) and **(C)** light (pink) were plotted against the ratio of Nc-0, AuNc-x and AgNc-x.

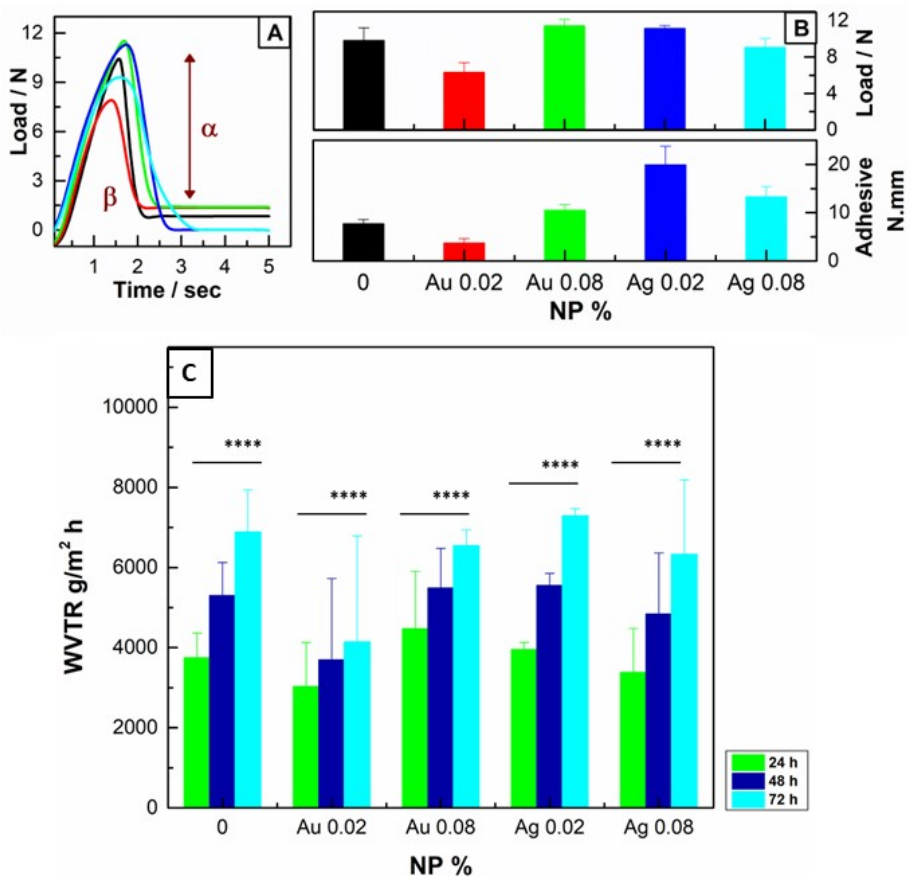

Figure S9. Adhesion tests of Nc-0, AuNc-x and AgNc-x gels at 37 ℃ on the Texture Analyzer. (A) Detachment profile (obtained from the force/distance curve), α is the maximum detachment force and β (area under the curve) is the total adhesion work, (B) plots of the detachment profile and total adhesion of Nc-0, AuNc-x and AgNc-x gels. (C) Water vapor transmission rate monitoring of Nc-0 and Nc-x hydrogels at 50% relative humidity and 37 ℃ after 24h, 48h and 72h.

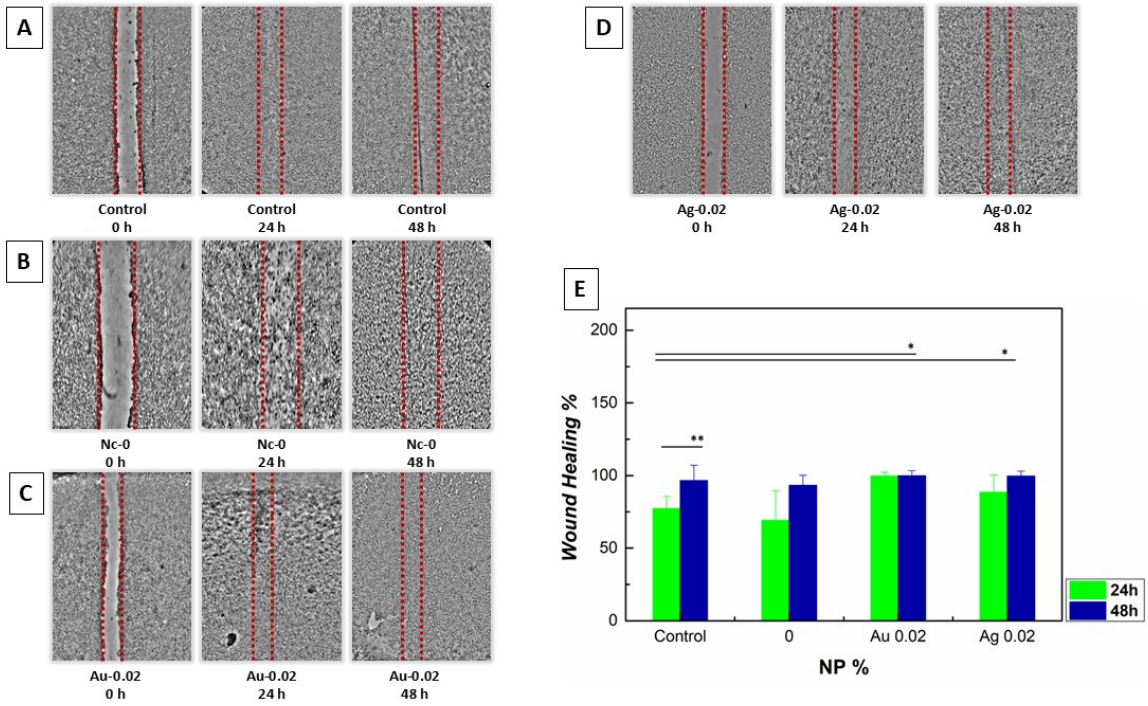

Figure S10. Microscope images showing the effects of (A) control, (B) Nc-0, (C) Au-0.02, (D) Ag-0.02 gels at t = 0, 24 and 48 hours on CCD-986Sk human skin fibroblast cells and (E) shows the percentage of wound healing with and without treatment.